Available online at www.sciencedirect.com
ScienceDirect
Journal of the European Ceramic Society 28 (2008) 2835–2843
www.elsevier.com/locate/jeurceramsoc

Investigation of the damage behaviour of refractory model materials at high temperature by combined pulse echography and acoustic emission techniques

G. Briche, N. Tessier-Doyen, M. Huger *, T. Chotard *

Groupe d'Etude des Matériaux Hétérogènes (GEMH, EA 3178), Ecole Nationale Supérieure de Céramique Industrielle, 47 à 73 Avenue Albert Thomas, 87065 Limoges Cedex, France

Received 4 March 2008; received in revised form 12 April 2008; accepted 18 April 2008
Available online 9 June 2008

Abstract

The understanding of the thermomechanical behaviour of high temperature castables is essential for their use as linings in high temperature furnaces and refining vessels in the metallurgical, cement, and petrochemical industries. The increasing use of the finite element calculations for the prediction of the behaviour in using conditions requires the knowledge of mechanical properties at high temperature and especially for model materials. This work deals with the characterisation of the damage behaviour during thermal cycling of two two-phase refractory model materials when considering thermal expansion mismatch between the constituents. The acoustic emission technique (AE) and the ultrasonic pulse echography technique, both carried out at high temperature, were applied as non-destructive characterisation methods to monitor the damage extension within the materials submitted to thermal stress and to follow the evolution of the associated elastic properties, respectively.

Keywords: Refractories; Thermal expansion; Mechanical properties; Damage; Ultrasonic techniques

1. Introduction

The heterogeneity of industrial refractory materials results from their composition involving multiphase materials such as aggregates of different sizes, bonding phases and various additives. The grains arrangement, the shape of aggregates and the microstructural flaws such as porosity and cracks, make difficult the prediction of the mechanical and thermal behaviours of such materials. These ones generally exhibit complex heterogeneous microstructures which can give rise to high internal thermal stresses. Because of thermal expansion mismatch or phase changes, the service conditions of these materials can greatly affect their initial microstructural state so as their thermomechanical properties.

The aim of this paper is to investigate the effect of thermal expansion mismatch on damage behaviour and consequently on elastic properties evolution of debonded and microcracked materials. Temperature variations can lead either to interfacial separation between aggregates and matrix or to microcracks, both depending on the range of CTE mismatch between phases. Such effects modify all the thermomechanical properties of the material, especially Young's modulus, strongly dependent on microstructure and composition. Firstly, typical Young's modulus temperature dependence of industrial refractories will be presented. Secondly, two model materials with different thermal expansion mismatches will be investigated by ultrasonic pulse echography (US echo) and acoustic emission technique (AE) conducted during high temperature thermal cycle. Finally, Young's modulus (E) evolutions will be correlated to AE activity variations considering the specific types of damage induced by CTE mismatch, respectively.

2. Untypical high temperature Young's modulus evolutions of industrial refractories

For refractory materials, their Young's modulus exhibits generally a typical hysteresis loop when the temperature varies[1–3] (Fig. 1a and b). At room temperature (after firing), the low value

* Corresponding authors.
E-mail addresses: marc.huger@unilim.fr (M. Huger), thierry.chotard@unilim.fr (T. Chotard).

0955-2219/$ – see front matter © 2008 Elsevier Ltd. All rights reserved.
doi:10.1016/j.jeurceramsoc.2008.04.023

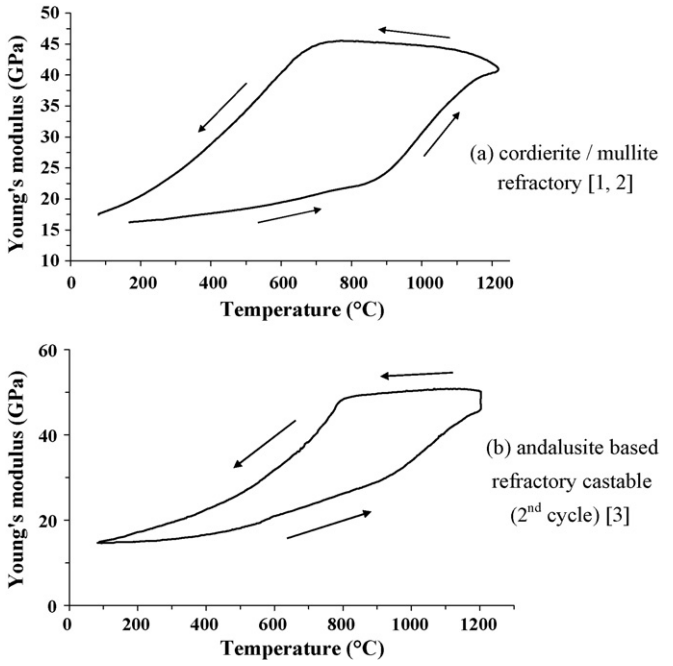

Fig. 1. Examples of Young's modulus evolution vs. temperature for different industrial refractory materials.

of the modulus is due to the internal damage induced by thermal expansion mismatch that occurs during the cooling stage of elaboration. Then, when temperature increases, the material resorbs this initial damage because the residual stresses due to the thermal expansion mismatch decrease gradually: thus, this mechanism leads to a progressive Young's modulus increase. During cooling, the vitreous phase, which promotes damage cure at high temperature, solidifies and the material keeps high elastic properties. Below a given temperature, the residual stresses level imposed by cooling generates damage again: the Young's modulus decreases and reaches a value close to its initial one.[4] Few papers have been published dealing with the temperature dependence of Young's modulus. Studying stable materials which do not suffer any structural nor microstructural transformations, Wachtman et al.[5] showed in 1961 that a regular and reversible decrease is generally observed in the Young's modulus vs. temperature plot, such a behaviour being imputed to the weakening of interatomic bondings. However, because of their coarse grains, heterogeneous and multiscale structure, refractories exhibit behaviours far from this prediction and, indeed, research works rather report an hysteresis loop shape for Young's modulus variations vs. temperature. For example, Case et al.[6] have observed hysteresis phenomena on anisotropic coarse grained alumina material and Nonnet et al.[7] so as Baudson et al.[8] have underlined similar behaviours for alumina castables and MgO/C refractories. These discrepancies, with the predictions given by the model of Wachtman et al.[5], are not always due to the same physical mechanisms. However most frequently they can be explained by the thermal expansion mismatch between the solid phases.

The case of alumina/carbon shaped refractories is also very interesting and can be here detailed. Ladle shrouds are components used in continuous steel casting to protect metal against oxidation. At the beginning of the process, these cylindrical parts (several tens of mm in thickness) are usually at room temperature when the molten steel, at temperature up to 1550 °C, suddenly flows inside. Al_2O_3/C refractories similar to those used for ladle shrouds have been studied.[9] They are composed of Al_2O_3 coarse grains and graphite flakes in a matrix bonded by a phenolic resin. Anti-oxidant compounds are added. After isostatic pressing, materials are fired at 1000 °C in inert atmosphere. Then, after firing, the material cohesion is ensured by the pyrocarbon resulting from the phenolic resin pyrolysis. When they are subjected to heating/cooling cycles, their Young's modulus exhibits a hysteretic evolution.

Fig. 2 shows the results of Young's modulus obtained for a 62 vol.% alumina composition sample during temperature cycles performed at 5 °C min^{-1} between 20 °C and 850 °C.

It can be noticed that the very low initial value of Young's modulus suited well to ladle shroud applications (especially thermal shocks[10]). In opposite, with stable fine ceramics which exhibit regular reversible E decrease when the temperature increases, strong non linear and irreversible effects are observed. The large increase from 450 °C to 650 °C can be attributed to the closure of interparticle, decoherences and cracks due to the thermal expansion mismatch. Regarding the CTE difference between the alumina grains and the carbon matrix, the presence of decoherences surrounding alumina grains seems to be responsible for this specific behaviour. When cooling, below 650 °C, Young's modulus decrease is due to decoherences and cracks opening. Such non-conventional behaviour is not easy to describe accurately because a lot of mechanisms, which can occur simultaneously, arise during the heating/cooling cycles. So, the influence of discontinuous interfaces and cracks is experimentally observable but remains difficult to analyse. Obviously, macroscopic Young's modulus phenomena are closely linked to the temperature behaviour of each constituent of the refractory material. But these constituents are generally numerous and their individual influences cannot be easily characterised.

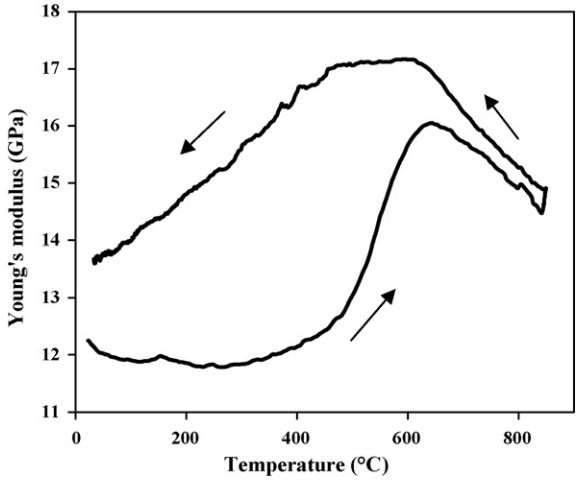

Fig. 2. Evolution Young's modulus vs. temperature for an Alumina/carbon refractory material.

The most convenient approach consists to reduce the microstructure to only two constituents (a matrix (m) and particles (p)). Indeed, it allows the study of two-phase model materials exhibiting simplified behaviours. Depending both on the sign of the CTE mismatch between the two phases ($\Delta\alpha = \alpha_m - \alpha_p$) and on the microstructure, various phenomena can occur when such a material is heated and cooled down (interfacial debonding, microcracking or adjusted interfaces).

3. Materials and methods

The studied two-phase samples contain randomly dispersed alumina particles whose physical and chemical characteristics are close to those of the aggregates used in industrial refractories previously presented. The main properties required for the binding phase are isotropy, homogeneity, to be inert and the possibility to adjust its thermal expansion according to the CTE of the inclusions. So, glasses were chosen because their coefficient of thermal expansion is easily adjustable by modifying the oxides proportions in their chemical composition.

3.1. Materials

Glass/alumina particles composite specimens are prepared using two different borosilicate glasses as matrix, which are referenced as G1 and G3 (Table 1). The dispersed phase is constituted of 99.9% pure alumina balls. For each two-phase system, a 15% controlled volume fraction of inclusions was added to fine glass powder. Organic additives are used to facilitate the shaping by cold uniaxial pressing of the mixture. After a binding removal treatment, a post hot pressing stage ($p = 15$ MPa, $T = T_g + 200\,^\circ$C) in a wolfram carbide die is performed in order to reduce the matrix porosity. Then specimens are naturally cooled to room temperature with a cooling rate of about $10\,^\circ\text{C min}^{-1}$.

Fig. 3 shows micrographs of polished surfaces of Alumina/G1 and Alumina/G3 specimens containing 15 vol.% of inclusions. The particles shape is not perfectly spherical and the Alumina/G1 system ($\alpha_m < \alpha_p$) shows a dark interfacial zone which can be due to a gap arising during cooling (Fig. 3a). For Alumina/G3 system ($\alpha_m > \alpha_p$) which exhibits greater CTE matrix, cracks in the matrix and around alumina inclusions can be optically observed using a fluorescent UV dye penetrant (Fig. 3b). The samples porosity is derived from the theoretical density (predicted from those of the two constituents) and density measurements performed by hydrostatic weighting. The remaining porosity being generally less than 1.5%, it may be though that cracks and debonding do not affect significantly the overall porosity.

3.2. High temperature ultrasonic pulse echography

The principal interest of this technique (US echo) described elsewhere[11] is to be able to follow the evolution of Young's modulus, which is directly related to the damage of the material, according to the temperature. A wideband pulse of ultrasonic compression wave is obtained by subjecting a magnetostrictive material to a magnetic field. The ultrasonic wave propagation through the studied materials is ensured by an alumina wave guide attached to the sample by refractory cement. This measurement is made in the configuration known as "long bar mode", i.e. that side dimensions D of the sample are low in front of the wavelength λ of the propagated wave (condition: $D/\lambda < 0.2$). Fig. 4 presents a scheme of the experimental setup used for high temperature pulse echography measurements. The Young's modulus, E, is calculated using the well known relationship:

$$E = \rho \cdot \left(\frac{2L}{\tau}\right)^2 \quad (1)$$

in which τ is the time delay between two successive echoes corresponding to a round-trip within the sample, L the sample length and ρ the material density. The great sensitivity of wave velocity to the material microstructure leads to calculated E effects which can be considered as pertinent behaviour indicators of multiphase materials at high temperature.

3.3. High temperature acoustic emission technique

Acoustic emission (AE) is defined as "the class of phenomena whereby transient elastic waves are generated by the rapid release of energy from localised sources within a material (or structure) or the transient waves so generated". When a material is submitted to stresses (such as mechanical stresses, electric transients, etc.), acoustic emission can be generated by a variety of sources, including crack nucleation and propagation, multiple dislocation slip, twinning, grain boundary sliding, Barkhausen effect (realignment or growth of magnetic domains), phase transformations in alloys, debonding of fibres in composite materials or fracture of inclusions in alloys.[12–17] It has been used either at the laboratory level or at the industrial scale. Usually, this technique is applied as a non-destructive characterisation technique in order to follow in real-time the evolution of the damage

Table 1
Thermo-elastic properties of the constituents

		Designation	E[a] (GPa)	Poisson's ratio, ν	α[b] ($\times 10^{-6}\,\text{K}^{-1}$)	$\Delta\alpha$ ($\times 10^{-6}\,\text{K}^{-1}$)	T_g (°C)
Dispersed particles	α-Alumina (99.9%)	Spherical (500 μm)	340	0.24	7.6	–	–
Glass	Amorphous	G1	68	0.20	4.6	−3.0	595
matrix	Amorphous	G3	72	0.23	11.6	4.0	470

[a] Measured at room temperature by ultrasonic pulse echography in infinite mode.
[b] Measured by dilatometric technique between 50 °C and 450 °C.

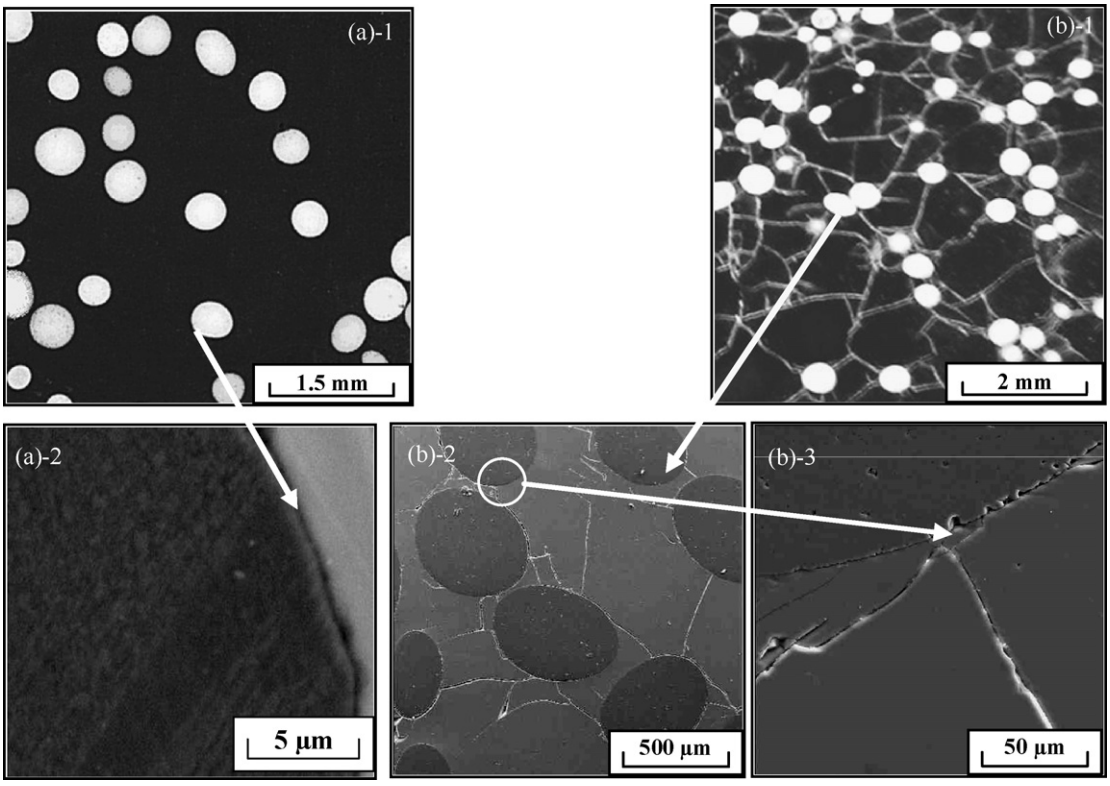

Fig. 3. Micrographs of 15 vol.% refractory model composite samples: (a) Alumina/G1, (b) Alumina/G3.

of a material subjected to mechanical loading.[18–21] Others new applications of this technique have been recently developed.[22,23] Here, the application of AE aims to characterise the damage or other microstructural transformations taking place in the material resulting from a particular thermal configuration.

The device of acquisition, rather similar to that of ultrasonic pulse echography, is composed of a wide band (175 kHz–1 MHz) sensor (PAC MICROPHONE µ80), a preamplifier (EPA 1220A) and an acquisition card associated with a computer (AEDSP-32/16 MISTRAS digital system from Physical Acoustics Corporation) showed in Fig. 5.The AE sensor is a major element of the chain of acquisition because it collects the whole of the signals induced by the elastic waves created within the material whose amplitudes are higher than a fixed threshold in order to amplify and to record them. This system allows the waveform and the main feature parameters well known in AE study such as count, hit, rise time, duration of hit, count to peak, amplitude (in dB), to be recorded. Fig. 6 presents different AE features extracted from the signal waveform.

A classical analysis of the evolution of the number of cumulated hits during the thermal cycle will be also carried out as well as a calculation of the hit rate according to the considered temperature:

$$R_T = \frac{d(\text{Hits})}{d(\text{temperature})} \quad (2)$$

with R_T in K^{-1} thermal cycling is the same for both US echo and AE testing. That means:

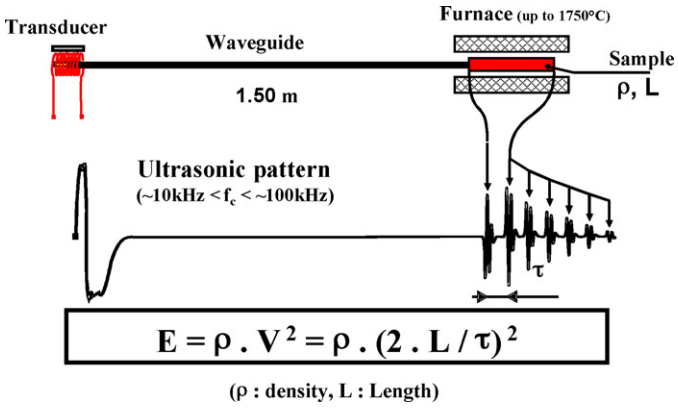

Fig. 4. Experimental setup used for Young's modulus measurement at high temperature by long bar mode pulse echography.

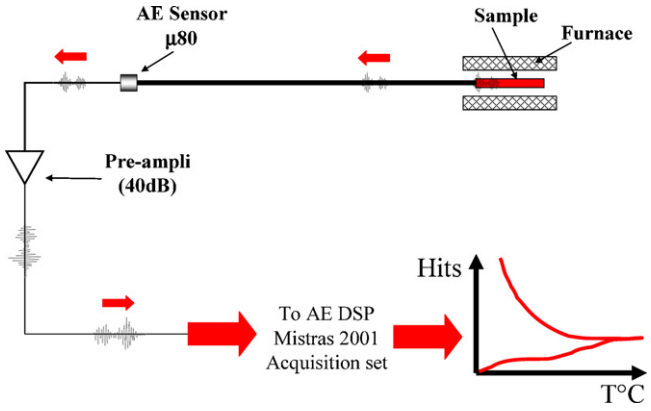

Fig. 5. Experimental setup used for high temperature acoustic emission measurements (AE).

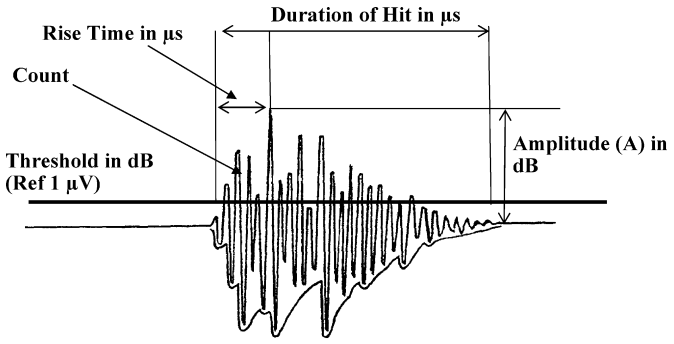

Fig. 6. Typical AE features extracted from the recorded signal (Hit).

- Heating at 5 °C min^{-1} from room temperature up to maximum temperature (depending on material).
- Dwell of 0.2 h at maximum temperature.
- Cooling at 5 °C min^{-1} from maximum temperature down to room temperature.
- Measurements performed above the glass softening point ($T_s > T_g$).

4. Results and discussion

4.1. Model material with interfacial debonding (Alumina/G1; $\Delta\alpha < 0$)

For this material, the thermal CTE mismatch between matrix and alumina particles is -3.0×10^{-6} K^{-1}. Fig. 7 shows the evolution of Young's modulus vs. temperature for Alumina/G1 composite. When heating, from room temperature to roughly 450 °C, a quite stable evolution of E is observed. Then, E value increases slowly up to 550 °C. This corresponds to the onset of the progressive closure of the interfacial debonding, most probably incomplete at this temperature. At 600 °C (close to T_g of G1 matrix) and onward, a notable decrease of the elastic properties of the specimen is observed. As the glass softening mechanism is predominant up to 820 °C, the two-phase material exhibits the matrix behaviour. At dwell temperature, the material reaches the condition to achieve the best interfacial contact between matrix and particles.

During cooling, between 820 °C and 600 °C, Young's modulus re increases noticeably. This fact is due to the stiffening of the matrix induced by the decrease of temperature. Below 600 °C and down to nearly 300 °C the elastic properties remain quite stable but have an upper value than the one quoted for the same temperature range during heating (80 GPa and 73 GPa, respectively). This observation confirms the healing of the damage during heating as occurred during the dwelling at 820 °C. Between about 300 °C and room temperature, the mechanical adhesion of interfaces decreases, decoherences open again and E falls down to reach its initial value.

If we look at the AE results (Fig. 8), some more information can be obtained. Firstly, regarding the evolution of the cumulated number of hits vs. temperature, we can quote that there is an acoustic activity both during heating and cooling stages. Obviously, the level of this activity is much greater during cooling than during heating (96% and 4% of the total amount of hit, respectively). However, as the AE technique is very sensitive to mechanisms occurring at local scales, the number of recorded hits during heating (<20) can be assumed as a significant one. Three major AE activity stages can be identified. During heating, the first one ranges from room temperature to 820 °C. Early during this period (up to 300 °C), the first AE bursts are more likely related to the setting of the contact between particles and matrix. It is important to remember that the CTE of the particles is higher than the one of the matrix and then the contact can occurs due to an higher expansion of the particles. It is also important to note that, as already observed in Fig. 3a, the surfaces of the particles are quite smooth. So, when contact with matrix occurs, this lack of asperities can explain the low level of recorded signals induced by this mechanism. Above G1 T_g (595 °C) and up to 820 °C, the glass softening mechanism is probably responsible of the very few number of recorded signals either because of the mechanism previously quoted (lack of asperities), or because of the attenuation of the acoustic waves.

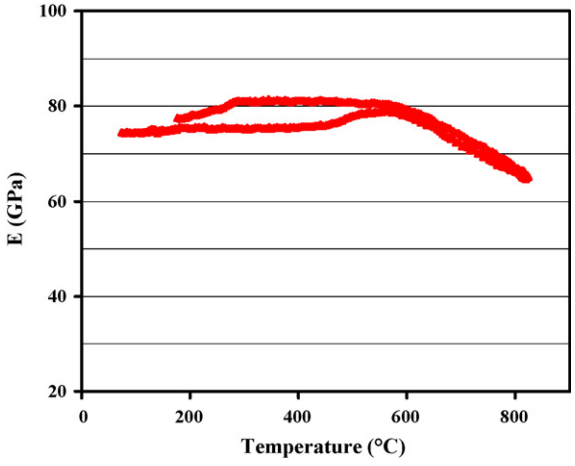

Fig. 7. Young's modulus evolution vs. temperature for Alumina/G1 composite ($\Delta\alpha < 0$).

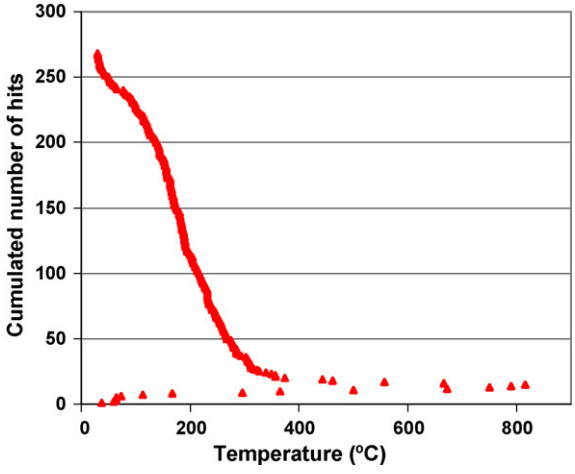

Fig. 8. Cumulated number of hits as a function of temperature during thermal cycling of Alumina/G1 composite ($\Delta\alpha < 0$).

The second period starts from the dwell temperature (820 °C) down to approximately 300 °C. During the first part of this temperature range (down to 380 °C) a very low AE activity is recorded. The hit rate (R_T) remains marginal. This shows that very few number of events occur and confirm that the material is cured of its damage. Above 380 °C, the AE activity evolves significantly, R_T notably increases. This fact shows that something appends at a local scale in the material. Indeed, even if it is not easily detectable on the E vs. temperature evolution (Fig. 7), AE evolution vs. temperature indicates that the onset of damage (decoherences) has already begin induced by the decrease of the interfacial adhesion. At this stage, from 300 °C to room temperature, AE activity strongly moves up. As already explain before, this temperature domain is characteristic of the re-opening of the interfacial cracks (decoherences) exhibiting a high level of AE associated to a notable drop of the elastic properties.

4.2. Model material with matrix microcracking (Alumina/G3; $\Delta\alpha > 0$)

Fig. 9 presents the evolution of Young's modulus vs. temperature for Alumina/G3 composite. As quoted in Fig. 3b, this material exhibits a matrix microcraking damage related to the positive CTE mismatch between its phases ($\Delta\alpha = 4.0 \times 10^{-6}\,K^{-1}$).

During heating stage, from room temperature up to G3 T_g (470 °C), E is quite constant. Then, a sudden increase of this characteristic, whereas matrix becomes viscous, is emphasised. The plateau and the following small decrease of E (from 500 °C to 640 °C) prove that a competition between the flaws resorption process (increase) and the matrix softening (decrease) occurs.

During cooling, from 640 °C to nearly 480 °C, and as observed for Alumina/G1 composite, the increase of E modulus linked to the stiffening of the glassy phase, suggests also that the microcracking healing stage is nearly complete as the sample has been previously heated at a temperature above the softening point. Below this last temperature down to roughly 180 °C, a small inflexion of the E vs. temperature curve can be detected. This progressive slight loss of elastic properties, within this temperature domain (relatively speaking), tends to demonstrate that a damage mechanism (matrix microcraking) has most probably begin to onset. Finally, from 180 °C to ambient temperature the tensile stresses applied to the matrix become overcritical and a large microcracking propagates in the glass matrix leading to drastic change in Young's modulus vs. temperature curves. The final E value indicates that the initial degree of microcracking is not fully recovered.

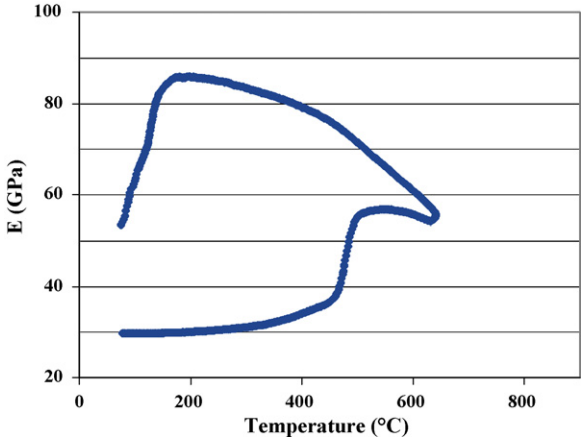

Fig. 9. Young's modulus evolution vs. temperature for Alumina/G3 composite ($\Delta\alpha > 0$).

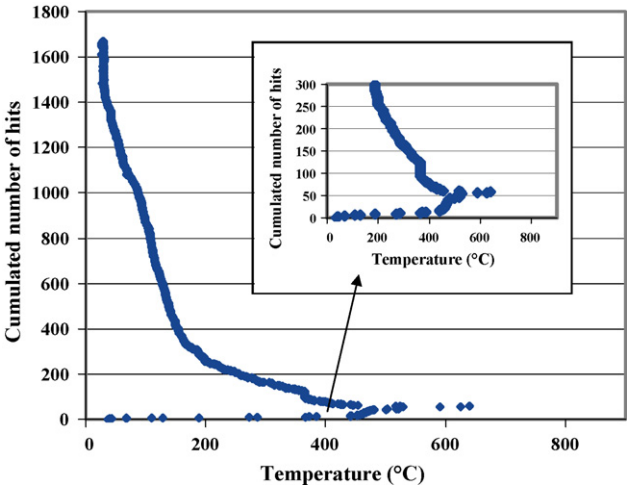

Fig. 10. Cumulated number of hits as a function of temperature during thermal cycling of Alumina/G3 composite ($\Delta\alpha > 0$). Magnification of the heating stage.

If we focus now on the AE cumulated number of hits vs. temperature presented in Fig. 10, one can say that, in a similar manner to Alumina/G1 composite, AE signals are recorded both during heating and cooling stages. However, the higher amount of hits acquired for Alumina/G3 composite clearly indicates that the damage phenomenon which takes place within the material is definitely more active (or higher in quantity) than the one quoted for Alumina/G1 composite. During heating period, a higher AE activity is marked (Magnification in Fig. 10). Early in this period (from ambient temperature to nearly G3 T_g (470 °C)), a very low level of AE activity is recorded. Then, above this temperature and for a very short range (40 °C max.), the hit rate suddenly rises significantly. As already said before, at this temperature, the matrix becomes viscous leading to a progressive but quite fast damage resorption phenomenon. The associated AE signals recorded are most likely related to the contact occurring between the surfaces of the microcracks due to the high CTE of the matrix compared to the one of particles ($11.6 \times 10^{-6}\,K^{-1}$ and $7.6 \times 10^{-6}\,K^{-1}$, respectively). Up to 640 °C, the AE activity becomes again marginal.

The beginning of the cooling stage is relatively similar to the end of the heating one. However, around 550 °C, a significant start of the AE activity is observed. It is important to note that this detection in AE is spotted at a higher temperature that the one for which the inflexion of the E curve obtained in ultrasonic echography has been observed (480 °C). During this temperature range (down to about 200 °C) the constant rate of AE activity tends to confirm that the damage process has occurred and gradually propagates within the material. Below nearly 200 °C, AE activity becomes highly intense. This strong burst in AE signals

suggests that a massive damage development has occurred and confirms the sudden loss of the elastic properties in this range of temperature (from 200 °C to ambient temperature).

4.3. Discussion and combined analysis

For a given volume fraction of alumina balls, E and its associated AE feature are more sensitive to matrix cracks damage process (Alumina/G3 with $\Delta\alpha > 0$) than to interfacial gaps damage one (Alumina/G1 with $\Delta\alpha < 0$). The development of such flaws can be explained by the thermal stresses level during cooling. When temperature varies, the hydrostatic pressure at the interface between the inclusion and the matrix can be expressed as:

$$p = \frac{(\alpha_m - \alpha_p)\,\Delta T}{(1-\nu_m)/2E_m + (1-2\nu_p)/E_p} \quad (3)$$

m and p subscripts denote the matrix and the particles, respectively. α stands for the thermal expansion coefficient, E for Young's modulus, ν for Poisson's ratio. ΔT represents the temperature cooling range over which the interfacial zone is free of stress.

Radial (σ_{rr}) and circumferential ($\sigma_{\theta\theta}$) stresses, respectively perpendicular and parallel to the interface, can be calculated according to:

$$\sigma_{rr} = -p \quad (4)$$

$$\sigma_{\theta\theta} = \frac{p}{2} \quad (5)$$

For negative $\Delta\alpha$ values, during cooling the matrix is subjected to radial tensile stresses whose magnitude can give rise to a debonding of the interface, this latter being postulated cohesive above T_g. The resulting interfacial gap (Fig. 11) can increase with the $\Delta\alpha$ range. On the contrary, positive $\Delta\alpha$ values subject the particle to a compressive stress state. So, the matrix endures radial compressive stresses and circumferential tensile stresses. The matrix plasticity being not able to accommodate the relative displacements, the arising of these circumferential tensile stresses leads to radial microcracking of the glass. AE technique can be particularly helpful in order to give a more precise interpretation concerning the chronology of the mechanisms. As an example, if we assume that, for the Alumina/G3 composite ($\Delta\alpha > 0$, matrix microcracking damage), the temperature, during the cooling stage, for which the early bursts of AE occur (nearly 550 °C), the associated value of the hydrostatic pressure p issued from Eq. (3) is about 52 MPa. This result, even if the damage process probably induces complex states of stress within the matrix and specifically near the matrix/particle interface, is very close (45 MPa) to the G3 matrix maximum bending strength obtained by three point bending test. Although AE technique must be applied carefully with respect to the type of material investigated and to the test carried out, this technique can allow the early detection of damage process associated with other non-destructive characterisation means (here US echography).

It may be thought that cracks propagation along interfaces can also be responsible for particles debonding in systems for which $\Delta\alpha > 0$. So, whatever the case is ($\Delta\alpha < 0$ or $\Delta\alpha > 0$), the defects induced by thermal stresses lead to Young's modulus decrease. Therefore, once such a decrease is observed during cooling, it is not possible to identify the type of defect responsible for this behaviour.

The proposed chronology of the phenomena acting during heating and cooling stages for the both materials are represented in Fig. 12. Fig. 12a presents the combined evolution of Young's modulus and AE feature (cumulated number of hits) vs. temperature for Alumina/G1 composite ($\Delta\alpha < 0$, decoherence damage process). Five different temperature domains can be identified and the proposed chronology can be as follow: at ambient

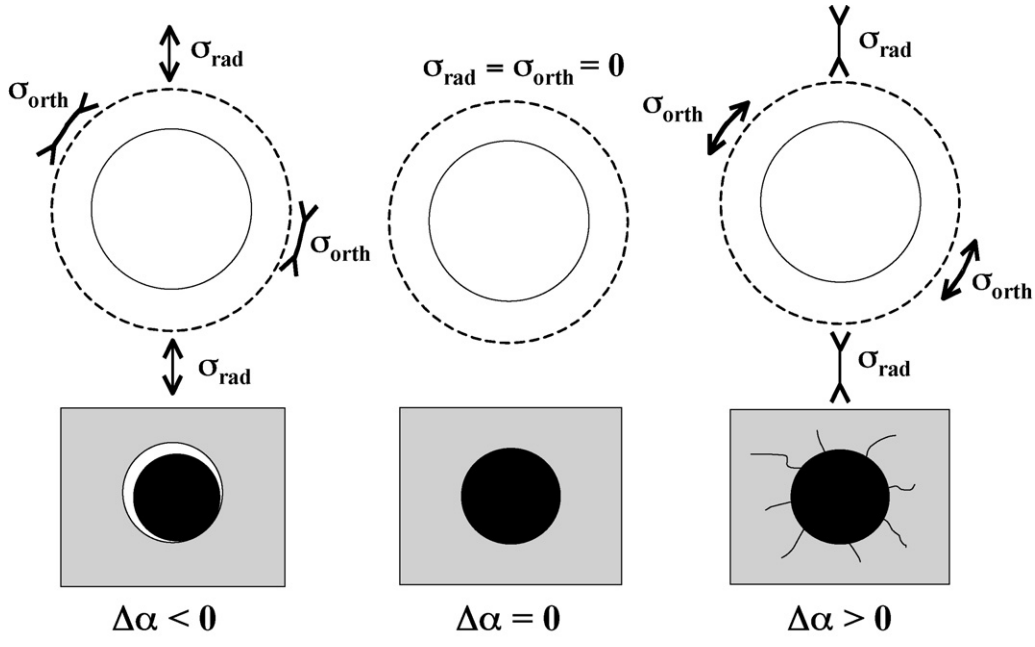

Fig. 11. Schematic representation of internal thermal stresses occurring during the cooling stage of a spherical inclusion embedded in an infinite isotropic phase.

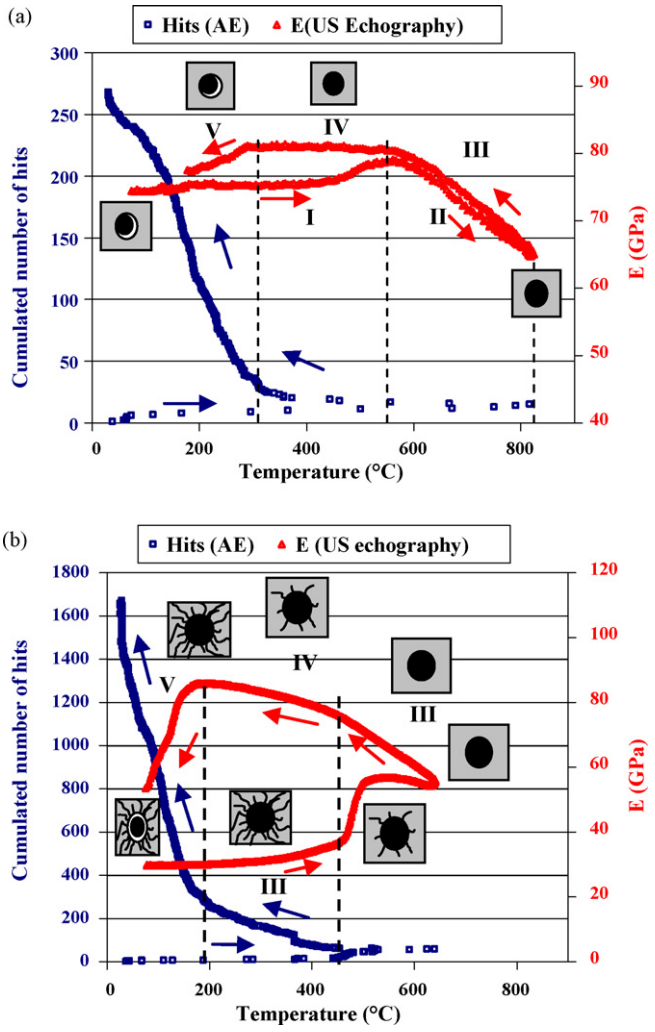

Fig. 12. Compared evolutions of AE feature and mechanical property as function of temperature: (a) Alumina/G1 ($\Delta\alpha < 0$), (b) Alumina/G3 ($\Delta\alpha > 0$).

temperature, the material, which has already been heated and cooled, of course during elaboration, is in its higher damaged state.

1. Stage I, progressive closure of the interfacial debonding has been engaged; stable evolution of E and very low AE activity corresponding most probably to the onset of contact between the particles and the matrix.
2. Stage II, from T_g to 820 °C: the two-phase material exhibits the matrix behaviour due to predominance of the glass softening mechanism: decrease of the elastic properties and AE activity is marginal at maximum temperature, recovering of the best interfacial contact between matrix and particles.
3. Stage III, from 820 °C to 600 °C: stiffening of the glassy phase during cooling; E increases, AE feature remains at a low level.
4. Stage IV: from 600 °C to 300 °C: intermediate temperature range where E remains quite stable with higher value (+10%) than the one quoted for the same temperature range during heating; this confirms the higher level of damage in the material before its cure at maximum temperature. However, AE activity recrudescence around 400 °C traduces the early stage of the damage onset.
5. Stage V: 300 °C to ambient: AE activity rises significantly, elastic properties drop, both traducing the beginning of a massive damage process.

The same kind of chronology can be proposed for the Alumina/G3 composite ($\Delta\alpha > 0$, matrix cracking damage process) but with few differences (Fig. 12b). As already explained for Alumina/G1 composite, the material is in its higher damaged state due to processing thermal cycle (heating then cooling stages):

1. Stage I, from ambient to 470 °C (G3 T_g): stable evolution of E associated with low AE activity (but higher than Alumina/G1 composite).
2. Stage II, from 470 °C to 640 °C: in the early part of the temperature range (470–510 °C), a strong rise of the elastic properties associated with a notable increase of AE features (number of hits and R_T) is observed. These evolutions denote the quite fast damage resorption phenomenon acting within the material due to the increase of the viscosity of the glassy phase. The associated AE signals recorded are most likely related to the contact occurring between the surfaces of the microcracks.
3. Stage III, cooling stage from 640 °C to 480 °C: as the same for Alumina/G1 composite, the stiffening of the glassy phase induces an increase of E. However, the early record of AE signal (nearly 550 °C) indicates that the matrix cracking damage process has already started in the material, but at a very local scale.
4. Stage IV: from 480 °C to 180 °C: slight inflexion of the E increase rate and strong rise of AE features (number of hits and R_T). Here, the recorded AE activity confirms the establishment of the damage process not so significantly marked on the Young's modulus evolution issued from US echo.
5. Stage V: From 180 °C to ambient, strong rise of AE feature associated to a big drop of the elastic properties. Generalised massive damage propagation.

5. Conclusion

Industrial refractories are highly heterogeneous multiphase materials: the size of their constituents can range from submicronic particles for binding phase powders to several millimetres for the biggest aggregates. Because of CTE disagreements, temperature variations induce microstructural changes leading to flaw evolutions. It has been shown that model materials (hot-pressed glass matrix containing spherical alumina inclusions) with various CTE mismatches can exhibit similar Young's modulus temperature effects than industrial refractories. The most significant results of this work are as follows:

- Young's modulus and associated AE features are highly sensitive to microstructural evolutions of multiphase materials.
- Young's modulus and AE activity evolutions of the studied two-phase model materials vs. temperature depend on the

CTE disagreement between matrix and inclusions and on the type of damage developed (higher AE activity for matrix microcracking).
- A very good correlation between AE and US pulse echography results is observed.
- The great sensitivity of the AE technique to detect phenomena at a very small scale within the material has been emphasised.

This study highlights the close correlation obtained between acoustic activity recorded during cooling and the loss of elastic properties determined by high temperature pulse echography technique. The difference in the AE cumulated activity is also quoted during heating and cooling stages. The combined used of this two ultrasonic techniques allows a chronology of both damage mechanisms onset and microcracks cure process to be proposed.

Acknowledgment

The authors want to thank the referee for his remarks which help them to improve the quality of this paper.

References

1. Soro, J., Bonnet J. P., and Huger, M., *Etude des propriétés physiques et thermomécaniques de matériaux réfractaires cordiérite/mullite* (in french). Internal Report, GEMH Laboratory, Limoges, France, 2005.
2. Chotard, T., Soro, J., Lemercier, H., Huger, M. and Gault, C., High temperature characterisation of Cordierite-Mullite refractory by ultrasonic means. *J. Eur. Ceram. Soc.*, 2008, **28**, 2129–2135.
3. Yeugo Fogaing, E., *Caractérisation à haute température des propriétés d'élasticité de refractaires électrofondus et de bétons réfractaires*. Ph.D. thesis, University of Limoges, France, 2006.
4. Tessier-Doyen, N., *Etude expérimentale et numérique du comportement thermomécanique de matériaux réfractaires modèles*. Ph.D. thesis, University of Limoges, France, 2003.
5. Wachtman, J. B., Telft, W. E., Lam, D. G. and Apstein, C. S., Exponential temperature dependance of Young's modulus for several oxides. *Phys. Rev.*, 1961, **122**, 1754–1760.
6. Case, E. D., Smyth, J. R. and Hunter, O., Microcracking in large-grain Al_2O_3. *Mater. Sci. Eng.*, 1981, **51**, 175–179.
7. Nonnet, E., Lequeux, N. and Boch, P., Elastic properties of high alumina cement castables from room temperature to 1600 °C. *J. Eur. Ceram. Soc.*, 1999, **19**, 1575–1583.
8. Baudson, H., Debucquoy, F., Huger, M., Gault, C. and Rigaud, M., Ultrasonic measurement of Young's modulus MgO/C refractories at High temperature. *J. Eur. Ceram. Soc.*, 1999, **19**, 1895–1901.
9. Vaudez, S., Huger, M. and Gault, C., Mechanical behaviour of Al_2O_3/c shaped refractories used in continuous casting. In *Proc. of the 6th Conf. of ECERS*, 1999, pp. 159–160.
10. Peruzzi, S., Vaudez, S., Huger, M., Gault, C., Glandus, J. C., Guillo, P. *et al.*, Thermomechanical modelling of alumina-graphite ladle shrouds used in continuous casting. In *Proc. of UNITECR '99*, 1999, pp. 128–132.
11. Huger, M., Fargeot, D. and Gault, C., High temperature measurement of ultrasonic wave velocity in refractory materials. *High Temp.-High Press.*, 2002, **34**, 193–201.
12. Hamstad, M. A., Thompson, P. M. and Young, R. D., Flaw growth in alumina studied by acoustic emission. *J. Acous. Emis.*, 1987, **6**, 93–97.
13. Bakuckas, J. G., Prosser, W. H. and Johnson, W. S., Monitoring damage growth in titanium matrix composites using acoustic emission. *J. Comp. Mater.*, 1994, **28**, 305–328.
14. Berkovits, A. and Fang, D., Study of fatigue crack characteristics by acoustic emission. *Eng. Fract. Mech.*, 1995, **51**, 401–416.
15. Havlicek, F. and Crha, J., Acoustic emission monitoring during solidification processes. *J. Acous. Emis.*, 1999, **17**, 3–4.
16. Coddet, C., de Barros, G. and Beranger, G., Influence of thermal cycling between 20 and 400 °C on the oxidation of copper. In *Proc. of the European Symposium*, 1981, pp. 417–426.
17. Coddet, C., Chretien, J. F. and Beranger, G., Investigation on the fracture mechanism of oxide layers growing on titanium by acoustic emission. *Titanium Titanium Alloys: Scient. Technol. Aspects*, 1982, **2**, 1097–1105.
18. Prosser, W. H., Jackson, K. E., Kellas, S., Smith, B. T., McKeon, J. and Friedman, A., Advanced waveform-based acoustic emission detection of matrix cracking in composites. *Mater. Eval.*, 1995, 1052–1058.
19. Barré, S. and Benzeggagh, M. L., On the use of acoustic emission to investigate damage mechanisms in glass-fibre-reinforced polypropylene. *Comp. Sci. Tech.*, 1994, **52**, 369–376.
20. Suzuki, H., Takemoto, M. and Ono, K., The fracture dynamics in a dissipative glass fibber/epoxy model composite with AE source simulation analysis. *J. Acous. Emis.*, 1996, **14**, 35–50.
21. Pauchard, V., Brochado, S., Chateauminois, A., Campion, H. and Grosjean, F., Measurement of sub-critical crack-growth rates in glass fibbers by means of acoustic emission. *J. Mater. Sci. Lett.*, 2000, **19**, 2141–2143.
22. Chotard, T., Smith, A., Rotureau, D., Fargeot, D. and Gault, C., Acoustic emission characterisation of calcium aluminate cement hydration at an early stage. *J. Eur. Ceram. Soc.*, 2003, **23**, 387–398.
23. Chotard, T., Quet, A., Ersen, A. and Smith, A., Application of the acoustic emission technique to characterise liquid transfer in a porous ceramic during drying. *J. Eur. Ceram. Soc.*, 2006, **26**, 1075–1084.